International Journal of Heat and Mass Transfer 196 (2022) 123273

Contents lists available at ScienceDirect

International Journal of Heat and Mass Transfer

journal homepage: www.elsevier.com/locate/hmt

Computational modelling of the local structure and thermophysical properties of ternary MgCl2-NaCl-KCl salt for thermal energy storage applications

Mickaël Lambrecht*, María Teresa de Miguel, María Isabel Lasanta, Gustavo García-Martín, Francisco Javier Pérez

Surface Engineering and Nanostructured Materials Research Group, Complutense University of Madrid, Complutense Avenue s/n, Madrid, Spain

ARTICLE INFO

Article history:
Received 11 March 2022
Revised 7 July 2022
Accepted 22 July 2022
Available online 27 July 2022

Keywords:
Concentrated solar power
Thermodynamic simulations
Molecular dynamics simulations
Heat transfer fluid
Local structure

ABSTRACT

Molten salts as heat transfer fluids (HTF) for concentrated solar power (CSP) plant application are considered as the best thermal storage medium, and more precisely molten chlorides, presenting a wide operating range and coupled with competitive cost. Furthermore, MgCl2-NaCl-KCl (MgNaK) mixture appeared as the most promising one but need further studies to better understand its thermophysical properties. Indeed, its hydrated form leads to the formation of corrosive compounds. In this research, two different methods are used to model the ternary mixture. The dehydration process is evaluated by thermodynamical calculations with Thermocalc software. Then, the local structure, thermal conductivity and viscosity are estimated by means of molecular dynamics simulation, with LAMMPS package. The results were close to past simulations studies and experimental references, but discrepancies need to be further minimized regarding some variable fluctuations.

1. Introduction

Producing renewable energy has become one of the major challenges of this decade and solutions are rising with the development of next generation CSP. Moreover, molten chlorides as HTF appeared to be the most promising thermal storage medium, presenting a high operating range and low cost. The most cost-effective and performant one is the ternary MgNaK chloride mixture, which provides a wide operating range [380ºC;750ºC] and low cost (0.35$/kg) [1]. Nevertheless, oxygen diffusion within the salt and hygroscopic magnesium chloride lead to the formation of corrosive hydroxyl compounds, such as MgOHCl, already described in past studies [2–7]. Computational simulations and thermodynamical calculations can be used to better understand its properties and evaluate the performance of such a mixture, in real plant. Indeed, these numerical methods must be validated by experimental testing, and are precursor of the development of future algorithmic models that could be implemented in new power plants, for automated machine learning and digital twins development. Molten chlorides have already been studied for CSP application and some of these results will be compared to our calculations [8–25]. Indeed, assessment of potassium and sodium alkali chloride were the most investigated ones [19, 21, 23, 24], but magnesium chloride [22] and the ternary MgNaK chloride [22, 25, 26] attract more attention as they became salts of interest, offering the support of experimental studies to the design of accurate phase diagrams.

The calculated phase diagram of MgNaK chloride has already been studied for research on optimal eutectic melting point. FactSage software calculations present three temperatures at 381.62ºC, 382.01ºC, and 382.45ºC for compositions of 64.47/38.19/21.21 wt%, 53.41/20.97/25.62 wt%, and 44.15/47.25/8.60 wt% respectively. Moreover, Coventry and al. assessed this phase diagram with a eutectic temperature of 383ºC with a composition of 55/24.5/20.5 wt% respectively [27], supported by experimental measurement.

In this paper, the life cycle of a ternary hydrated-MgNaK salt have been analyzed with computational thermodynamics methods, from the necessary hexahydrate magnesium chloride ($MgCl_2{\cdot}6H_2O$) dehydration process before its use in a CSP plant; as described in a previous review [1]; to its determining thermophysical properties as a heat transfer fluid. First, compounds activities and site fractions of the hydrated ternary mixture have been calculated with the use of Thermocalc software, to better understand its evolution with an inert and aerobic atmosphere. Then,

* Corresponding author.
E-mail address: milambre@ucm.es (M. Lambrecht).

https://doi.org/10.1016/j.ijheatmasstransfer.2022.123273

the local structure of dehydrated molten chlorides at different temperatures were performed by molecular dynamic simulations with open source LAMMPS (Large-scale Atomic/Molecular Massively Parallel Simulator) package. To validate this method, the temperature range was selected based on previous simulations and experimental studies.

2. Methodology

2.1. Thermodynamic simulation

Thermocalc Software was used with CALPHAD (CALculation of PHAse Diagrams) methodology for predicting thermodynamic, kinetic, and other properties of multicomponent material systems with the "Compound Energy Formalism" (CEF), detailed by Hillert [28]. Plus, SGTE Molten Salt Database permitted to perform the calculations. The Gibbs free energy of phases is computing with a good short range order accuracy, as it deals with its phase constituents (*pc*), such as neutral atoms, ions, or vacancies within the sublattices (*s*) [29]. Indeed, a phase is described by the site fraction (y) summation of its phase constituents $\sum y_{pc}^{s}$. Then, extremal species of each sublattices are defined as end-members (*em*) and their weighted average define a surface of reference (*sr*). (Equation 1)

$$G_{em}^{sr} = \sum G_{end}^{0} \prod y_{pc}^{s} \tag{1}$$

Moreover, Gibbs free energy values of end-members compounds are relative to standard state Gibbs energy of the number (m) of components (i) present in the end-members sublattices (Equation 2).

$$\Delta_f^0 G_{em} = G_{end}^{0} - \sum G_i^{standard} \sum m^s \tag{2}$$

Furthermore, the ideal entropy of mixing is considered (Equation 3).

$$-ST = RT \sum_s n^s y_{pc}^s \ln\left(y_{pc}^s\right) \text{ with } \begin{Bmatrix} n \text{ the stoechiometric coefficient} \\ R \text{ the gas constant coefficient} \\ T \text{ the temperature} \\ S \text{ the entropyof mixing} \end{Bmatrix} \tag{3}$$

2.2. Molecular dynamic simulations

Molecular dynamic simulations were performed with open source LAMMPS package [30]. The micro-canonical ensemble (NVE) represents an isolated system without exchange of particles or energy with the environment, and a constant volume. This ensemble was used to verify rapidly the stability of the system.

Harmonic bond (bs) and angle (as) style were used with the respective potentials

$$E_{bs} = \frac{K_{bs}(r - r_0)^2}{2} \text{ with } \begin{Bmatrix} K_{bs} \text{ a prefactor } \left(\frac{eV}{Angstr\ddot{o}\ m^2}\right) \\ r_0 \text{ the equilibrium bond distance } (Angstr\ddot{o}\ m) \end{Bmatrix} \tag{4}$$

$$E_{as} = \frac{K_{as}(\theta - \theta_0)^2}{2} \text{ with } \begin{Bmatrix} K_{as} \text{ a prefactor } (eV) \\ \theta \text{ the equilibrium angle value } (Degree) \end{Bmatrix} \tag{5}$$

Lennard Jones potential was used for the force field of $MgCl_2$ equation (6) where ε and σ were estimated from the Lorentz-Berthelot rules equation (7), and the Born-Mayer-Huggins or Tosi/Fumi potential was used for (Na, K) Cl interactions equation (8), with coulombic interactions equation (9). The combination rules thrive to approximate the potential interaction between non-bonded atoms. The validity of the Lorentz-Berthelot rule is assumed as the atoms are modelized as hard spheres, and the potentials used in this study come from previous calculations by ab-initio molecular dynamics present in the literature [19, 31-33]. gathered on Table 1. The limitation of the force field accuracy could stem from the Lorentz-Berthelot mixing rule, as some deviations were pointed out by Boda and Henderson [34], depending on the size parameter. Plus, the cut-off radius was fixed as half of the system length, to minimize beyond potentials effects.

Table 1
Pair-potential parameters of the system

Pair	$A_{i,j}$ (eV)	ρ (Å)	$\sigma_{i,j}$	$C_{i,j}$ (eV.Å^6)	$D_{i,j}$ (eV.Å^8)
Na-Na	0.2637	0.3170	2.34	1.0486	0.4993
Na-Cl	0.2110	0.3170	2.755	6.9905	8.6758
Na-K	0.2636	0.3170	2.633	3.9860	0.2777
K-Cl	0.2109	0.3367	3.048	29.9467	45.5439
K-K	0.2636	0.3367	2.926	15.1605	14.9733
Cl-Cl	0.1582	0.3170	3.17	72.4021	145.4283
Pair		r_c (Å)		ε (eV)	
Mg-Mg		3.021		0.0048	
Mg-Na		2.565		0.0114	
Mg-K		2.906		0.0121	
Mg-Cl		3.947		0.0099	

$$E = 4\varepsilon\left[\left(\frac{\sigma}{r}\right)^{12} - \left(\frac{\sigma}{r}\right)^{6}\right] \text{ with } \begin{Bmatrix} \varepsilon \text{energy } (eV) \\ \varepsilon\,(Angstr\ddot{o}\ m) \\ \varepsilon\,(Angstr\ddot{o}\ m) \end{Bmatrix} \tag{6}$$

$$\begin{Bmatrix} \sigma_{ij} = \frac{1}{2}\left(\sigma_{ii} + \sigma_{jj}\right) \\ \varepsilon_{ij} = \sqrt{\varepsilon_{ii}\varepsilon_{ij}} \end{Bmatrix} between\ atom\ types\ i\ and\ j \tag{7}$$

$$E = Ae^{\left(\frac{\sigma - r}{\rho}\right)} - \frac{C}{r^6} + \frac{D}{r^8} \text{ with } \begin{Bmatrix} r_c \text{ the cut} - off \text{ distance} \\ \sigma,\ interaction - dependent\ length\ parameter \\ \rho,\ ionic - pair\ dependent\ lenght\ parameter \end{Bmatrix} \tag{8}$$

$$E_{coul} = \frac{q_i q_j}{r_{ij}} \text{ with } \begin{Bmatrix} q_i,\ q_j \text{ the charges of } i,\ j \text{ ions} \\ r_{ij} \text{ the separation distance of } i \text{ and } j \end{Bmatrix} \tag{9}$$

Partial radial distribution function (PRDF) was computed to study the local structure of molten chlorides at different temperatures following equation (10). Indeed, it describes the density probability of a pair of atoms with distance from a reference particle. Thus, the coordination number can be easily deduced equation (11).

$$g_{\alpha\beta}(r) = \frac{dN_{\alpha\beta}(r)}{r^2 dr} \cdot \frac{1}{4\pi\rho_\beta r^2} \text{ with } \begin{Bmatrix} \rho_\beta \text{ the density of } \beta \text{ species} \\ N_{\alpha\beta} \text{ the number of } \beta \text{ in an sphere of center } \alpha \\ r \text{ the distance from } \alpha \end{Bmatrix} \tag{10}$$

$$N_{\alpha\beta} = 4\pi\rho_\beta \int_0^{r_{min}} g_{\alpha\beta}(r) r^2 dr \text{ with } \{r_{min} \text{ the first peak distance in the PRDF }\} \tag{11}$$

The simulation box is set to periodic boundary conditions, to make the atoms exiting from a box side re-enter from the other side.

2.3. Equilibrium Molecular Dynamics - Green-Kubo method

This method computes viscosity with an average of stress/pressure tensor auto-correlation function, which can be calculated in an equilibrated simulation, with a continuous momentum flow. Indeed, thermal conductivity is similarly calculated with three arguments per atom: kinetic energy, potential energy, and stress with formula:

$$\kappa = \frac{V}{3k_B T^2} \int_0^{\infty} J(0) \cdot J(t)\, dt \text{ with } \begin{Bmatrix} V \text{ the volume of the system} \\ k_B \text{ the Boltzmann constant} \\ T \text{ the temperature} \\ J \text{ the heat flux} \end{Bmatrix} \tag{12}$$

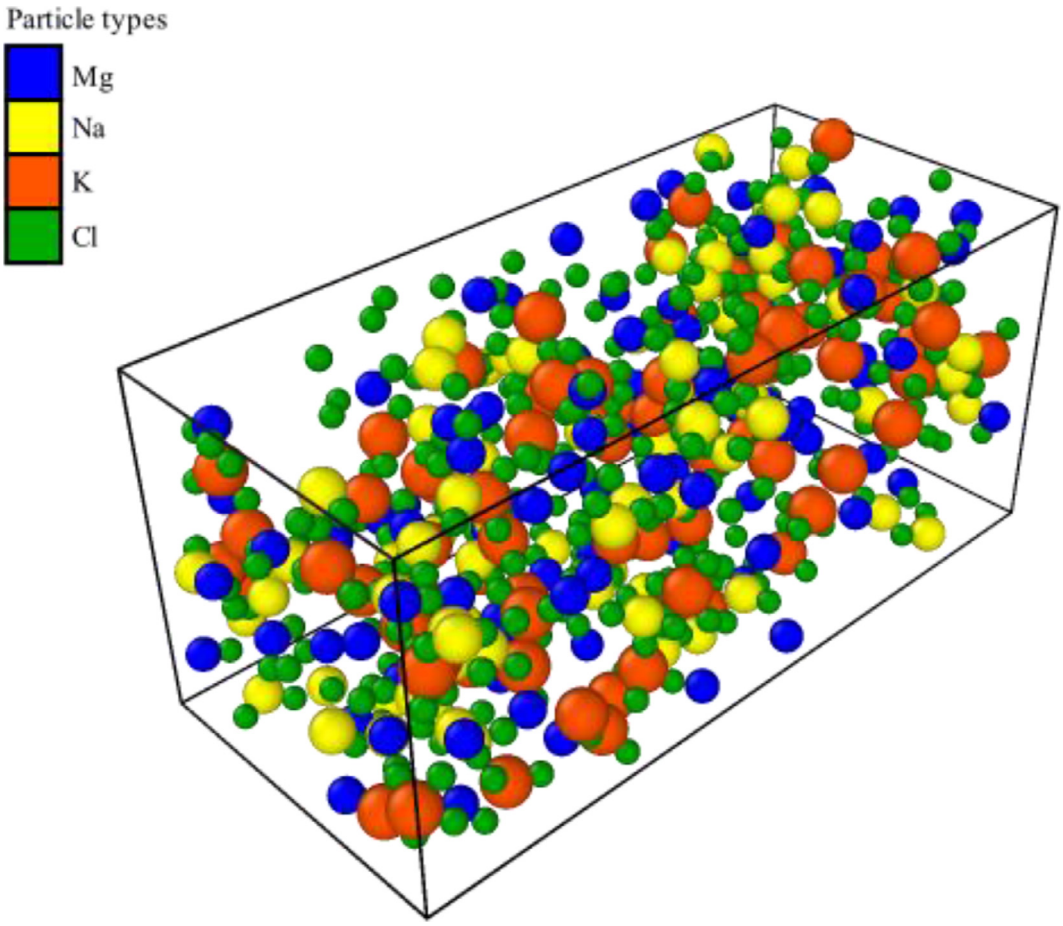

Figure 1. Screenshot of the simulation box of (MgNaK)Cl

All simulations were performed with different sizes of boxes, respectively with 216, 512, and 1800 atoms for single chlorides, with first NPT equilibration followed by NVT equilibration, for 100ps each. A mean was then calculated, and discrepancies are represented by error bars. The mean error of the thermostat was 48K. For $MgCl_2$-NaCl-KCl mixture, a system with 40/30/30 %mol was computed. A screen of the simulation box with 648 atoms is showed on Figure 1. The calibrations and validations of the different models has been made with references of experimental values and comparing with past simulations.

3. Results and discussion

3.1. Phases evolution of hydrated MgNaK chloride

The dehydration process of MgNaK chloride have been analyzed through the computation of its amount of phase with temperature, compounds activities and site fractions.

As seen on Figure 2, the dehydration process is observable as multiple steps at 100ºC, 200ºC, 260ºC, identifiable as stages I, II and III (reactions (13), (14), (15)).

$$Stage\ I: \ MgCl_2 \cdot 6H_2O \rightarrow MgCl_2 \cdot 4H_2O + 2H_2O \quad (13)$$

$$Stage\ II: \ MgCl_2 \cdot 4H_2O \rightarrow MgCl_2 \cdot 2H_2O + 2H_2O \quad (14)$$

$$Stage\ III: \ MgCl_2 \cdot 2H_2O \rightarrow MgCl_2 \cdot H_2O + H_2O \quad (15)$$

Moreover, MgOHCl is already forming at 100ºC, and its conversion into MgO is predicted at 460ºC, confirmed by experimental DSC measures [1]. At 480ºC, MgOHCl is totally converted into MgO, leading to HCl formation and thus the increase of the gas phase.

When considering the liquid state of this mixture, two main structures are remarkable, the halite, present from 260ºC to 650ºC, and the ionic liquid, above this temperature. Indeed, in a CSP plant, a HTF must demonstrate relatively stable properties and a quantitative known behavior considering its thermophysical and thermodynamical aspects. To operate in a power plant, salt purification by dehydration is the most cost-relevant choice for molten chlorides. Nevertheless, this option cannot assure a total elimination of hydrates, as they react to form hydroxyl group and non-volatile species. Indeed, the first simulation on Figure 2 permits to estimate a maximum relative amount of magnesium-hydroxychloride of 10%. Thus, to simulate this contamination, dehydrated (MgNaK)Cl was computed with 10% MgOHCl at input, and activities of monoclinic NaCl, MgOHCl, $MgCl_2{\cdot}6H_2O$ and NaOH with respect to temperature on Figure 3. The activity of a phase is directly calculated from its thermodynamic potential, and the site fraction is the summation of the component in each sublattices of the system.

Firstly, magnesium chloride hydration is forming at ambient temperature with MgOHCl presence as its activity rises, whereas the successive steps of dehydration can be observed with $MgCl_2{\cdot}H_2O$ curve from 50 to 510ºC. Indeed, the activity increases linearly at each step, but the derivative diminishes, as the temperature range to dissociate a pair hydrate-magnesium increase when the coordination is lower (hexa- to tetra- to di- and mono-hydrate); the thermodynamic potential favors less complexed MgCl2. Then, MgOHCl activity decreases after 510ºC, only

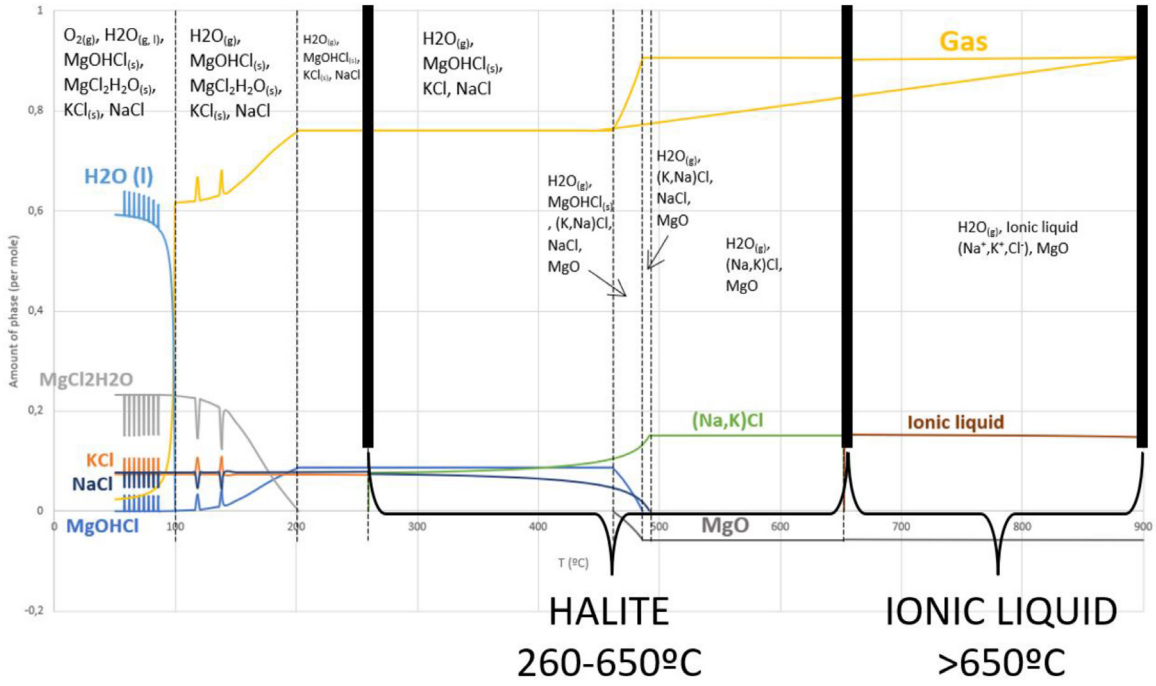

Figure 2. - Phases evolution of hydrated MgNaK chloride taken from reference [1].

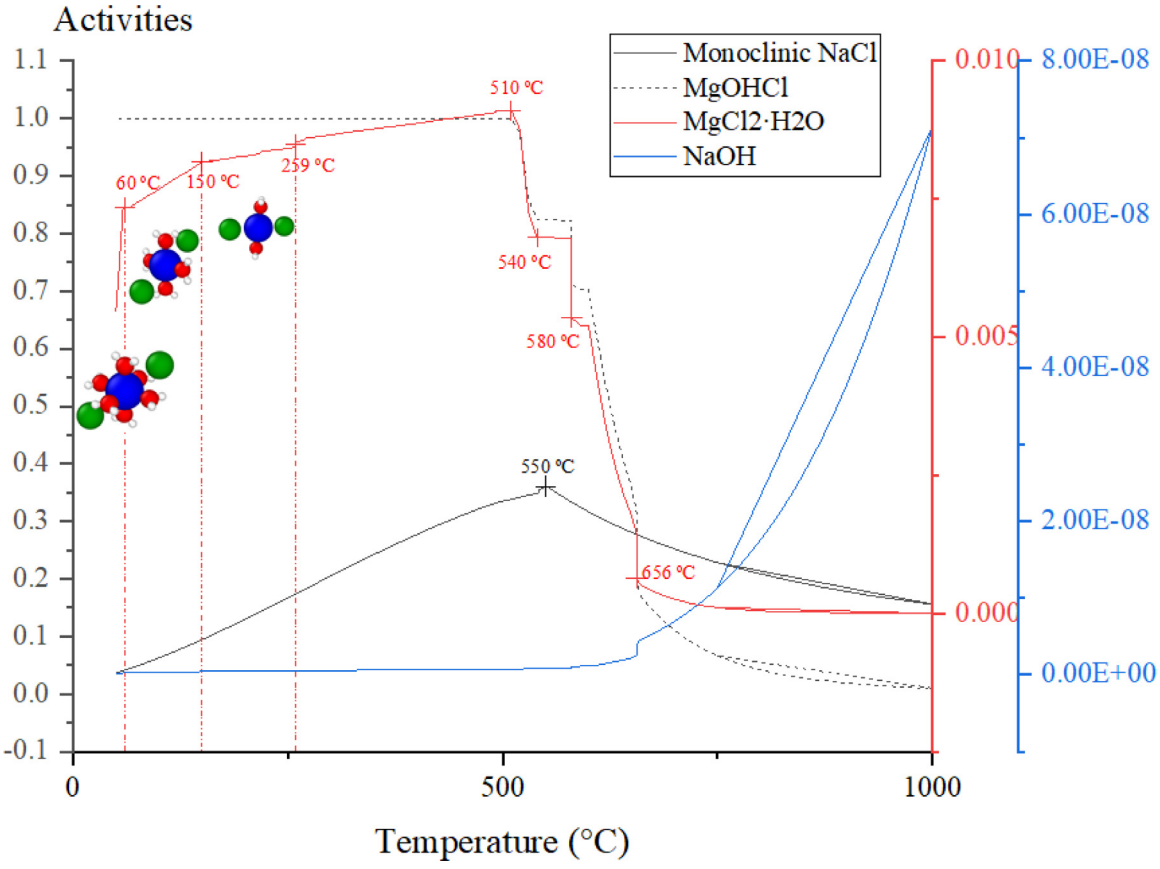

Figure 3. Activities of formed components in MgNaK chloride

when total dehydration occurred and are followed by two plateaus at 540ºC and 580ºC. Furthermore, NaOH activity increase at 656ºC coming from hydroxide-free ionic potential favoring the reaction with sodium chloride at high temperature, which is identified as ionic liquid. This formation could lead to a mitigation of hydroxide-induced corrosion in the CSP plant at high temperatures.

To better understand and visualize the transition between halite and ionic liquid phases, a dehydrated (MgNaK)Cl system was com-

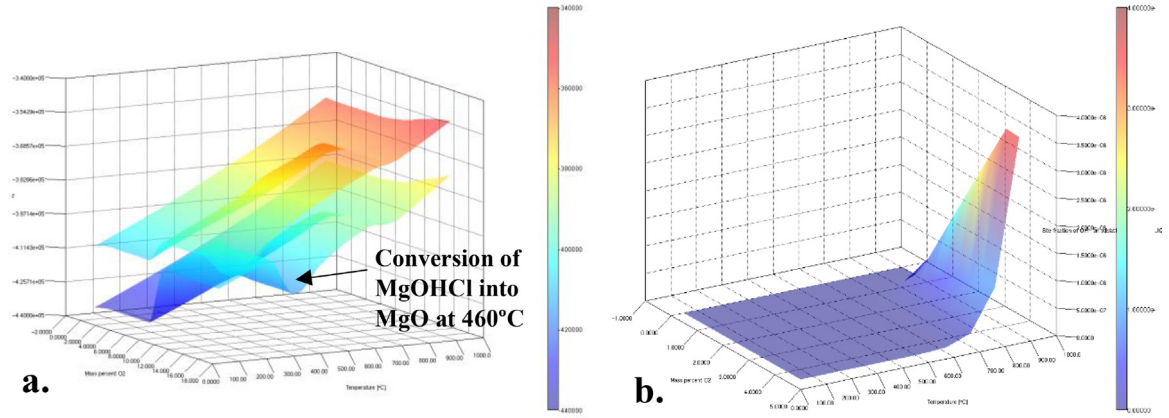

Figure 4. Site fraction of OH groups in MgNaK chloride under a. air atmosphere (halite and ionic phase) and b. nitrogen atmophere (overall system)

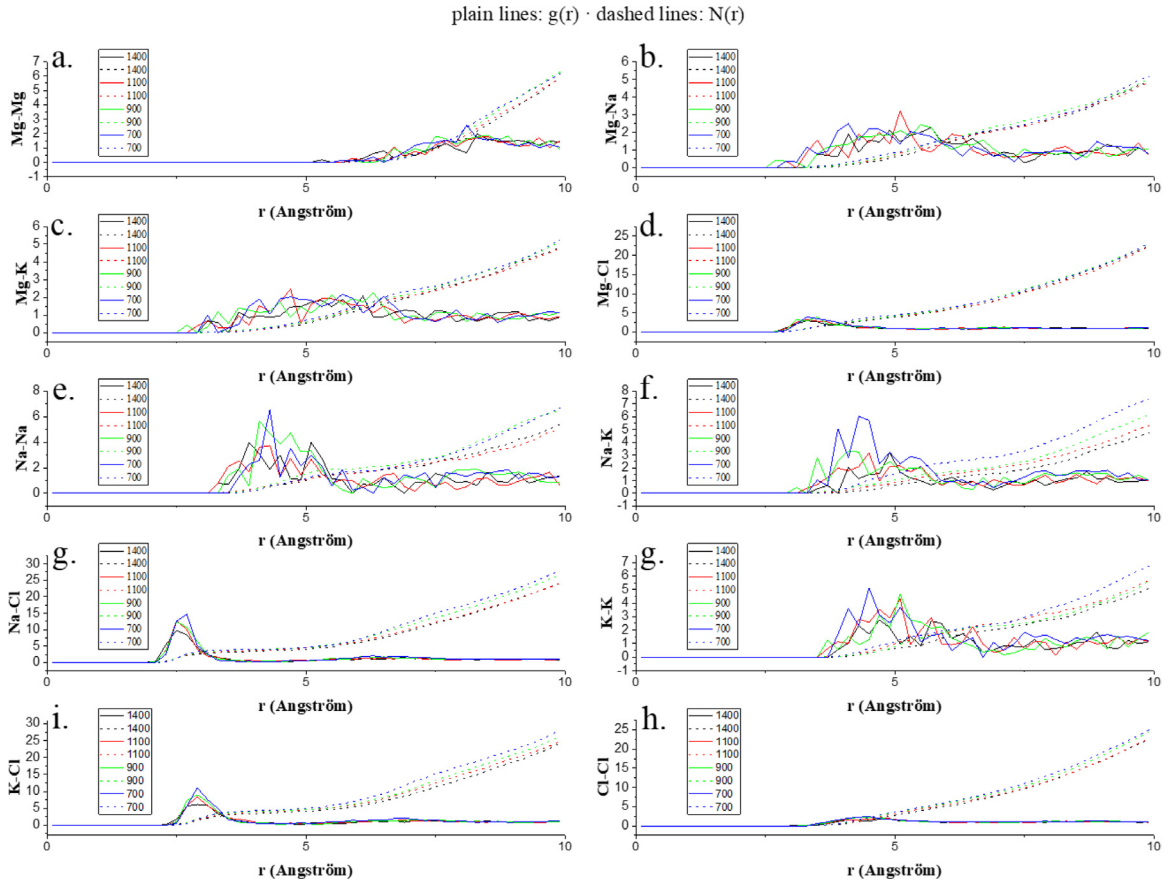

Figure 5. Partial distribution function and coordination number of ion-pairs distances in MgNaK chloride with temperature

puted with an initial amount of 10% of MgOHCl, in aerobic and inert atmosphere. Hydroxyl site fraction calculations were performed for each phase and merged on the same graph, with respectively halite (lower function) and ionic liquid (upper function), on Figure 4. First, the site fraction of hydroxyl group has been calculated within an aerobic atmosphere, on Figure 4a. OH fraction is constantly increasing with temperature, as having a direct source from air inward diffusion into the liquid. Then, MgOHCl conversion to MgO is well defined at 450ºC in the halite domain, as OH site fraction is decreasing. Secondly, on Figure 4b, the same system was computed but under a nitrogen atmosphere and the calculations presented a much better behavior as OH site fraction is stable and nearly null under 700-750ºC. Moreover, it can be approximated that a maximum of 5 wt.% oxygen in nitrogen atmosphere can be acceptable, under 750ºC CSP conditions.

3.2. Molecular dynamic simulations

3.2.1. Local structure

Molecular dynamics were studied to analyze the local structure of the ternary MgNaK chloride and the influence of temperature. Thus, as explained in Section 2.2, it can be analyzed by the distribution of ions pair distances. PRDF and coordination numbers are plotted on Figure 5 and the first peaks of each pair are gathered on Table 2.

Table 2
First peak of ion-pairs distances with temperature

	700K	900K	1100K	1400K	Maximum relative variation
r_{min} (Mg-K)	**3.1**	**2.7**	**3.1**	**3.1**	**13%**
r_{min} (Mg-Na)	**2.9**	**2.7**	**2.9**	**3.5**	**21%**
r_{min} (Mg-Cl)	**3.3**	**3.1**	**3.3**	**3.3**	**6%**
r_{min} (Na-Na)	**3.9**	**3.5**	**3.5**	**3.3**	**15%**
r_{min} (Na-K)	**3.5**	**3.1**	**3.9**	**3.7**	**11%**
r_{min} (Na-Cl)	**2.7**	**2.5**	**2.5**	**2.5**	**7%**
r_{min} (K-K)	**4.1**	**3.7**	**3.9**	**4.3**	**10%**
r_{min} (K-Cl)	**2.9**	**2.9**	**2.9**	**2.7**	**7%**
r_{min} (Cl-Cl)	**4.5**	**4.1**	**4.1**	**4.1**	**9%**

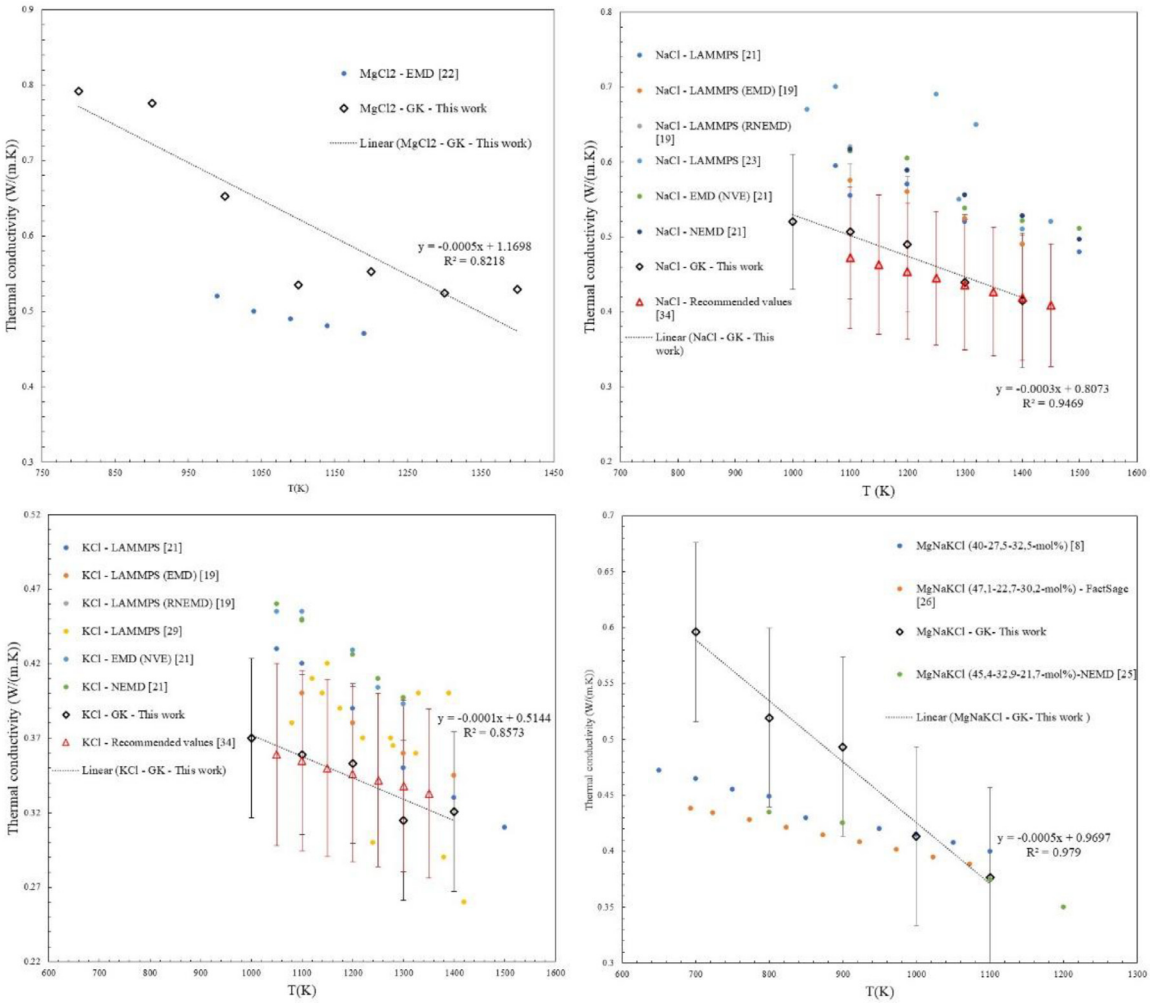

Figure 6. Calculated thermal conductivities compared to past research for a. MgCl2, b. NaCl, c. KCl and d. MgNaK chloride at different temperature

The first peaks of ions-pair distance show a higher disorder when varying temperature between positive-charged particles with a maximum relative variation of 21% for Mg-Na pair. The lower variation appeared to be with Mg-Cl pair, with 6%, coming from a higher density of chlorine atoms. Indeed, Na-Cl and K-Cl are the second lowest with 7% variation. Na-Cl, Na-Na, and Cl-Cl first peaks positions of 2.5, 3.3, and 4.1 Å at 1400K showed a good agreement of anion-cation pair, compared to experimental results of Edwards and al., at 2.6, 3.7, and 3.8 Å respectively under 1340K [35]. Plus, K-Cl first peak at 2.9 Å also showed a similar result with 3.1 Å in the work of Allen and al. [36], while magnesium local structure did not appeared to be studied experimentally. The disorder of the local structure can be easily observed with the coordination number curves, which decrease with temperature. Indeed, the probability of a structural stability decrease with the number of different interactions in a system. Also, the mobility of Mg atoms enhances the statistical path of Mg ions on near to the surface leading to the adsorption and inward diffusion of oxygen atoms. Therefore, atmosphere relative humidity must then be mitigated for high temperature applications, as being the source of oxygen contamination.

3.2.2. Thermal conductivity

Single salts and ternary (MgNaK)Cl have been computed with the Green Kubo method, in the same range of temperature of previous research to compare the results, gathered on Figure 6. Plus, experimental values have been taken as a reference [37]. Several simulations have already been performed on potassium and sodium chlorides in previous research [9, 21, 23, 24, 38, 39], with

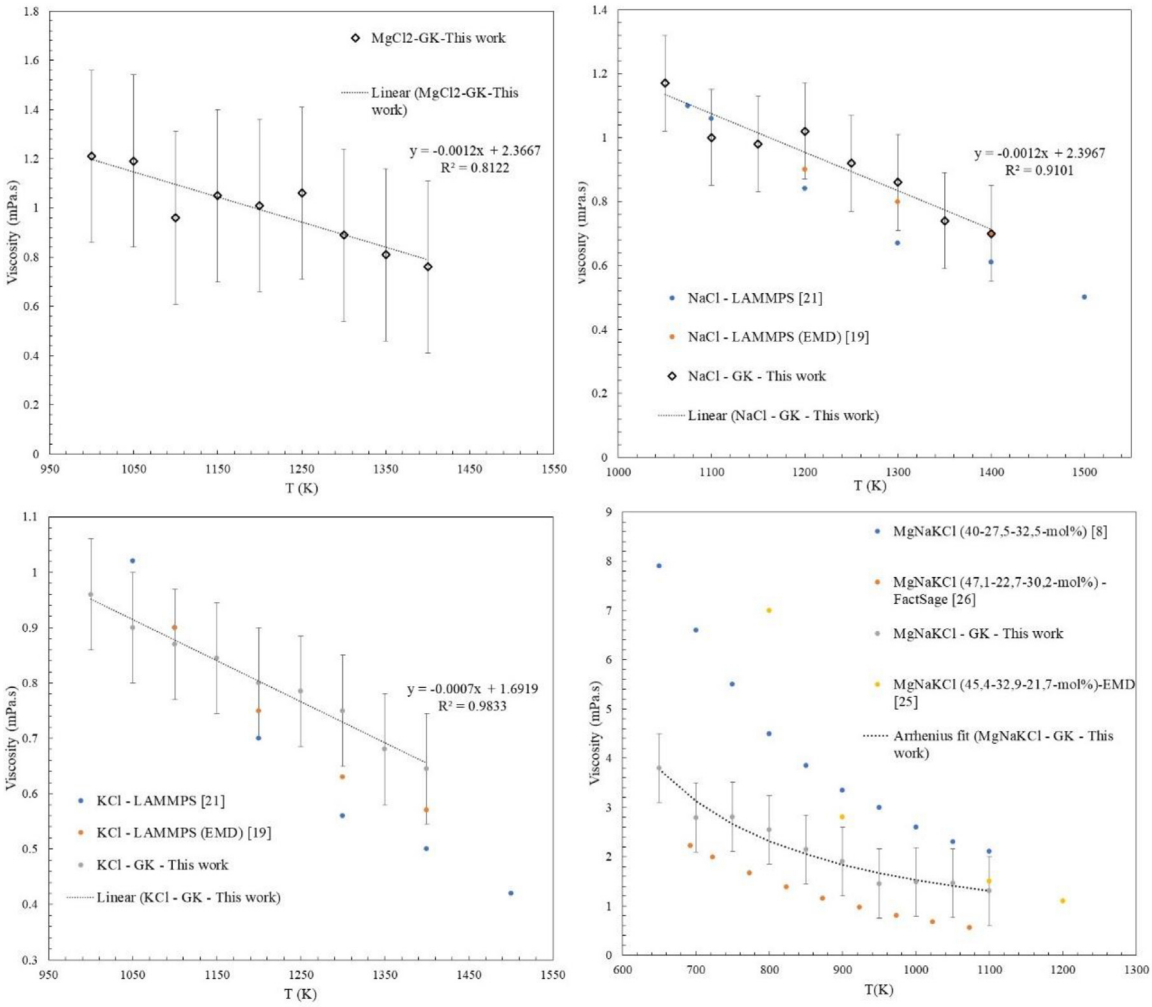

Figure 7. Calculated viscosities compared to past research of a. MgCl2, b. NaCl, c. KCl and d. MgNaK chloride at different temperatures

values between 0.7 and 0.48 W/(mK) for NaCl and 0.46 and 0.26 W/(mK) for KCl, from 1000K to 1400K. Moreover, most of the results present a linear behavior for all salts. Nevertheless, the overall discrepancy between each thermal conductivity curve of a same salt can be misleading for comparison. Indeed, variation in parameters such as timestep, swap rate, running time, box size or temperature control, added to a different algorithm resolving method, can rapidly lead to different values. Thus, an experimental reference was used for NaCl and KCl. For $MgCl_2$, much less research have been made and only one case of equilibrium simulation is found in the literature, with linear values between 0.52 and 0.47 W/(mK) for a temperature range from 975 K to 1200 K [22]. Finally, for the ternary MgNaK chloride, previous studies computed it with a round hard sphere method for a 40-27.5-32.5 mol% salt in a range of [650K; 1100K][8], non-equilibrium molecular dynamics [25], and we also compared these values considering FactSage calculations [26]. All our models show a thermal conductivity decreasing with temperature, confirming past investigations [8-20, 22], and MgNaK chloride linear regression showed a coefficient determination of 0.979. Plus, discrepancies occurred when varying the box system resulting in the error values, but the results are included in the error range given by reference. Furthermore, the uncertainty of the temperature is estimated to 30 degrees for the three single salts and 45 degrees for the ternary salt. Indeed, $MgCl_2$ high value at low temperature seems overestimated, and induced the strong temperature dependance of the ternary salt. This can be explained by the local pressure fluctuation term that induce a variation in the phonon-phonon collision probability. Then, each end-member of the system presents a different phonon mean free path. Moreover, a phonon free path higher than the interatomic distance increases the mass fluctuation term, and thus thermal conductivity, as demonstrated by Gheribi and Chartrand [40].

3.2.3. Viscosity

Green-Kubo formalism was performed on single and ternary MgNaK salts, and results are gathered on Figure 7. Chloride salts' viscosity have been studied by simulations, but no data was found on single $MgCl_2$. In our work, it showed a decreasing linear curve with temperature, as NaCl and KCl, whereas they presented an exponential trend in the range [1000K; 1400K] and [1050K; 1400K] respectively in past studies [19, 21]. Nevertheless, the ternary MgNaK mixture showed an exponential form with a strong coefficient of determination (R^2=0.959) but is coherent with the results reported by Vignarooban and al [3] and Zhang, Salanne and al. [25]. Moreover, an Arrhenius regression fitted to the results, with the following form and parameters.

$$\eta = Ae^{B/T}, \ with \begin{Bmatrix} A = 0.2823 \\ B = 1684.4 \end{Bmatrix}$$

Indeed, coordination numbers of each pair showed a structural disorder with temperature, charge interactions becoming weaker,

Table 3
Linear regression of thermal conductivity and viscosity of single and ternary chloride salt calculated

Molten salt	Thermal conductivity – Regression equation	R^2	Viscosity – Regression equation	R^2
NaCl	y = -0,0003x + 0,8073	0,9469	y = -0,0012x + 2.3967	0,9101
KCl	y = -0,0001x + 0,5144	0,8573	y = -0,0007x + 1.6919	0,9833
$MgCl_2$	y = -0,0003x + 1,1698	0,8218	y = -0,0012x + 2.3667	0,9636
(MgNaK)Cl	y = -0,0005x + 0,9697	0,979	$y = 0{,}2823.e^{(1684{,}4/x)}$	0,959

inducing an increase in fluidity. Both thermal conductivity and viscosity most accurate regressions for each system are available on Table 3, with their respective coefficient of determination.

4. Conclusions

Thermo-molecular dynamic simulations were performed on single and ternary MgNaK chloride to study their local structure and physical properties with respect to temperature. First, the dehydration process of the magnesium hexahydrate chloride is computed, and activities of hydroxyl-compounds are highlighted, with the conversion of MgOHCl into solid MgO at 460ºC and an increase in NaOH activity after 656ºC. This NaOH potential formation at high temperature could lead to a mitigation of OH^--induced metal oxidation in a CSP plant. Moreover, the importance of an inert atmosphere such as nitrogen is confirmed as no corrosive OH-associated compound reaches equilibrium and forms within the salt. Indeed, from thermodynamic calculations, an estimated relative oxygen percent of 5% can be stated as a limit for CSP application at 750ºC in molten chloride, assuming punctual failures in the inertization system. Partial radial distribution was computed and confirmed the increase of structural disorder with temperature highlighted by a coordination number increasing slower. Then, the negative derivative of thermal conductivity and viscosity with temperature is confirmed and the values are close to experimental data and past simulation studies, as well as the Arrhenius behavior of the MgNaK chloride in viscosity. Physically, this decreasing is relatable with the molecule expansion when heating up. Nevertheless, an overestimation of thermal conductivity has been associated with the local pressure fluctuation influencing the phonon-phonon collision occurrence with temperature. Plus, the discrepancies occurring with respect to other research need to be minimized with more data to make accurate decision in future algorithmic models. Further research needs to be made on the interaction of chloride salts with nanoparticles to study and calculate their potential properties enhancement, and on the assessment of these results, to potentially link molecular dynamics and calphad methods.

Data availability

The data that support the findings of this study are available from the corresponding author, Mickaël Lambrecht, upon reasonable request.

Author statement

M. Lambrecht: Conceptualization, Validation, Writing – Original Draft, Writing – Review & Editing, Visualization **M.T. de Miguel:** Conceptualization, Validation, Investigation, Writing – Review & Editing, Visualization, Project administration **M.I. Lasanta:** Conceptualization, Methodology, Validation, Investigation, Project administration **G. García-Martín:** Resources, Writing – Review & Editing, Project administration **F.J. Pérez:** Conceptualization, Supervision, Funding acquisition

Declaration of Competing Interest

The authors declare the following financial interests/personal relationships which may be considered as potential competing interests:

Data Availability

Data will be made available on request.

Acknowledgments

This work received funding from the Agencia Estatal de Investigation in the frame of the "Proyectos I ± D ± I 2020" program and under project reference number PID2020-115866RB-C22 (PID2020-115866RB-C22/AEI/10.13039/501100011033).

Reference

[1] M. Lambrecht, et al., Past research and future strategies for molten chlorides application in concentrated solar power technology, Solar Energy Materials and Solar Cells 237 (2022) 111557.
[2] Z. Zhang, et al., The dehydration of MgCl2·6H2O by inhibition of hydrolysis and conversion of hydrolysate, Journal of Analytical and Applied Pyrolysis 138 (2019) 114–119.
[3] K. Vignarooban, et al., Heat transfer fluids for concentrating solar power systems – A review, Applied Energy 146 (2015) 383–396.
[4] H. Sun, et al., Assessment of effects of Mg treatment on corrosivity of molten NaCl-KCl-MgCl2 salt with Raman and Infrared spectra, Corrosion Science 164 (2020) 108350.
[5] W. Ding, et al., Molten chloride salts for high-temperature thermal energy storage: Continuous electrolytic salt purification with two Mg-electrodes and alternating voltage for corrosion control, Solar Energy Materials and Solar Cells 223 (2021) 110979.
[6] Y. Zhao, J. Vidal, Potential scalability of a cost-effective purification method for MgCl2-Containing salts for next-generation concentrating solar power technologies, Solar Energy Materials and Solar Cells 215 (2020) 110663.
[7] Q. Huang, et al., Thermal decomposition mechanisms of MgCl2·6H2O and MgCl2·H2O, Journal of Analytical and Applied Pyrolysis 91 (1) (2011) 159–164.
[8] Y. Li, et al., Survey and evaluation of equations for thermophysical properties of binary/ternary eutectic salts from NaCl, KCl, MgCl2, CaCl2, ZnCl2 for heat transfer and thermal storage fluids in CSP, Solar Energy 152 (2017) 57–79.
[9] W. Liang, G. Lu, J. Yu, Theoretical prediction on the local structure and transport properties of molten alkali chlorides by deep potentials, Journal of Materials Science & Technology 75 (2021) 78–85.
[10] S. Wu, H. Peng, L. Xie, Design and investigation of the novel ZnCl2 based ternary chloride salts with low-temperature for sensible energy storage, Applied Thermal Engineering 171 (2020) 114917.
[11] A.D. Pathak, et al., First-principles study of chemical mixtures of CaCl2 and MgCl2 hydrates for optimized seasonal heat storage, J. Phys. Chem. (2017) 16.
[12] S. Zhang, Y. Yan, Melting and thermodynamic properties of nanoscale binary chloride salt as high-temperature energy storage material, Case Studies in Thermal Engineering 25 (2021) 100973.
[13] G.C.Q. Pan, et al., Molecular simulations of the thermal and transport properties of alkali chloride salts for high-temperature thermal energy storage, International Journal of Heat and Mass Transfer 103 (2016) 417–427.
[14] A.E. Gheribi, J.A. Torres, P. Chartrand, Recommended values for the thermal conductivity of molten salts between the melting and boiling points, Solar Energy Materials and Solar Cells 126 (2014) 11–25.
[15] N.S. Venkateswara Rao Manga, Stefan Bringuier, Pierre Lucas, Pierre Deymier, Krishna Muralidharan, Interplay between structure and transport properties of molten salt mixtures of ZnCl2–NaCl–KCl: A molecular dynamics study, The Journal of Chemical Physics (2016) 12.
[16] N.S. Venkateswara Rao Manga, Joshua Paul, Saivenkataraman Jayaraman, Pierre Lucas, Pierre Deymier, Krishna Muralidharan, Molecular dynamics simulations and thermodynamic modeling of NaCl–KCl–ZnCl2 ternary system, CALPHAD: Computer Coupling of Phase Diagrams and Thermochemistry (2014) 8.
[17] L. Xu, et al., Microstructural and diffusive properties of Cr solute in MgCl2–NaCl–KCl eutectic: A First-Principles molecular dynamics study, Journal of Molecular Liquids 341 (2021) 117321.

[18] G. Pan, et al., A DFT accurate machine learning description of molten ZnCl2 and its mixtures: 2. Potential development and properties prediction of ZnCl2-NaCl-KCl ternary salt for CSP, Computational Materials Science 187 (2021) 110055.
[19] J. Ding, et al., Theoretical prediction of the local structures and transport properties of binary alkali chloride salts for concentrating solar power, Nano Energy 39 (2017) 380–389.
[20] J. Wu, et al., Molecular dynamics simulation on local structure and thermodynamic properties of molten ternary chlorides systems for thermal energy storage, Computational Materials Science 170 (2019) 109051.
[21] J. Wang, et al., Molecular Dynamics Simulations of the Local Structures and Transport Coefficients of Molten Alkali Chlorides, The Journal of Physical Chemistry B 118 (34) (2014) 10196–10206.
[22] A.E. Gheribi, A.T. Phan, P. Chartrand, A theoretical framework for reliable predictions of thermal conductivity of multicomponent molten salt mixtures: KCl–NaCl-MgCl2 as a case study, Solar Energy Materials and Solar Cells 236 (2022) 111478.
[23] K. Takase, I.A.N. Ohtori, Temperature dependence of thermal conductivity in molten alkali metal halides by MD simulation, ECS Proceedings, 99 (41) (2000) 376–382.
[24] N. Galamba, C.A. Nieto de Castro, Equilibrium and nonequilibrium molecular dynamics simulations of the thermal conductivity of molten alkali halides, The Journal of Chemical Physics (2007) 126.
[25] W. Zhou, Y. Zhang, M. Salanne, Effects of fluoride salt addition to the physico–chemical properties of the MgCl2–NaCl–KCl heat transfer fluid: A molecular dynamics study, Solar Energy Materials and Solar Cells 239 (2022) 111649.
[26] C. Villada, et al., Engineering molten MgCl2–KCl–NaCl salt for high-temperature thermal energy storage: Review on salt properties and corrosion control strategies, Solar Energy Materials and Solar Cells 232 (2021) 111344.
[27] G. Mohan, et al., Assessment of a novel ternary eutectic chloride salt for next generation high-temperature sensible heat storage. Energy Conversion and Management, 2018. 167: p. 156-164.
[28] M. Hillert, The compound energy formalism, Journal of Alloys and Compounds 320 (2) (2001) 161–176.
[29] L. J.O. Andersson, H.T. Höglund, P.F. Shi, B. Sundman, Computational tools for materials science, Calphad 26 (2002) 273–312.
[30] A.P. Thompson, et al., LAMMPS - a flexible simulation tool for particle-based materials modeling at the atomic, meso, and continuum scales, Computer Physics Communications 271 (2022) 108171.
[31] J.L.F.A. M. Zeron, C. Vega, A force field of Li+, Na+, K+, Mg2+, Ca2+, Cl−, and SO4 2- in aqueous solution based on the TIP4P/2005 water model and scaled charges for the ions, The Journal of Chemical Physics (2019) 17.
[32] N. Ohtori, M. Salanne, P.A. Madden, Calculations of the thermal conductivities of ionic materials by simulation with polarizable interaction potentials, The Journal of Chemical Physics 130 (10) (2009) 104507.
[33] Xinxing ZHANG, P.A.-L. Gregory A, CHASS and Devis DI TOMMASO1, *Interatomic potentials of Mg ions in aqueous solutions: structure and dehydration kinetics*, Eur. J. Mineral. (2018) 13.
[34] D. Boda, D. Henderson, The effects of deviations from Lorentz–Berthelot rules on the properties of a simple mixture, Molecular Physics 106 (20) (2008) 2367–2370.
[35] F.G. Edwards, The structure of molten sodium chloride, J. Phys. C: Solid State Phys. 8 (1975) 3483.
[36] D.A. Allen, The structure of molten zinc chloride and potassium chloride mixtures, J. Phys.: Condens. Matter 4 (1992) 1407.
[37] C.D. Chliatzou, et al., Reference Correlations for the Thermal Conductivity of 13 Inorganic Molten Salts, Journal of Physical and Chemical Reference Data 47 (3) (2018) 033104.
[38] Janz, G.J., Allen, C.B., Bansal, N.P., Murphy, R.M., Tomkins, R.P.T.,, Physical properties data compilations relevant to energy storage. II. Molten salts: data on single and multi-component salt systems. . U.S. Department of Commerce/National Bureau of Standards, NSRDS-NBS 61, Part II, 1979.
[39] Nagasaka, Y., Nakazawa, N., Nagashima, A.,, *Experimental determination of the thermal diffusivity of molten salts.*1992.
[40] A.E.G.a.P. Chartrand, Thermal conductivity of molten salt mixtures: Theoretical model supported by equilibrium molecular dynamics simulations, THE JOURNAL OF CHEMICAL PHYSICS 144 (2016) 084506 2016.